

The nonlinear growth of a gravitationally unstable interface in a Hele-Shaw cell

By T. MAXWORTHY

Departments of Mechanical and Aerospace Engineering, University of Southern California,
Los Angeles, CA 90089–1453, USA

(Received 8 August 1985 and in revised form 14 August 1986)

We report observations of the nonlinear growth of an unstable interface in a large Hele-Shaw cell in which it is possible, in the most extreme case, to follow the emergence of a single ‘finger’ from approximately thirty initial wavelets. The larger ‘fingers’ that emerge undergo further instability to form a highly contorted interface. We have measured a number of the averaged characteristics of this interface and can relate the various cases studied through length and time scales constructed from the independent parameters of the problem. We show that the most distorted interfaces may have a fractal dimension at scales larger than the instability wavelength and discuss the significance of this possibility.

1. Introduction

There has been a recent increase in interest in the problem of interface motion in a Hele-Shaw cell (see Tryggvason & Aref 1983, hereinafter referred to as TA; Aref & Tryggvason 1984; Park, Gorell & Homsy 1984; Park & Homsy 1984; McLean & Saffman 1981, among others) following the fairly steady advances in knowledge which resulted from the seminal papers of Saffman & Taylor (1958), Saffman (1959) and Taylor & Saffman (1959). This interest is motivated mainly by the analogy to the flow of fluid in a porous medium as outlined particularly well in TA and Wooding & Morel-Seytoux (1976), with the most important practical situation being the attempt to displace oil in an oil field by pumping water into a secondary well. In all of these latter papers, one of the more interesting observations concerns the emergence of a single, smooth finger of intruding, less-viscous fluid in the relatively narrow channels used in the experiments. My own interest is of long standing, having been first aroused when a student by the observation of ‘bubble competition’ and the eventual dominance of one or two of the growing wavelets in the dynamically similar case of Rayleigh–Taylor instability by a fellow student B. C. Watson, as published by Emmons, Chang & Watson (1960). Observations in a Hele-Shaw cell, reported here, (see, also, Wooding & Morel-Seytoux 1976 & TA for example) and in finger growth in a turbulent stratified fluid (Liu, Maxworthy & Spedding, 1985) have made it clear that the phenomenon is ubiquitous and deserves further study under the simplest possible circumstances where a great deal of experimental data can be extracted relatively accurately by elementary but labourious techniques. Also, in many situations where Rayleigh–Taylor instability occurs (e.g. inertially driven fusion experiments) there is considerable interest in being able to scale the growth rate of the nonlinear, unstable interface which forms. Despite extensive numerical calculations, there is still considerable uncertainty over the long-time behaviour of such interfaces. Experiments in this area are notoriously hard to perform owing to

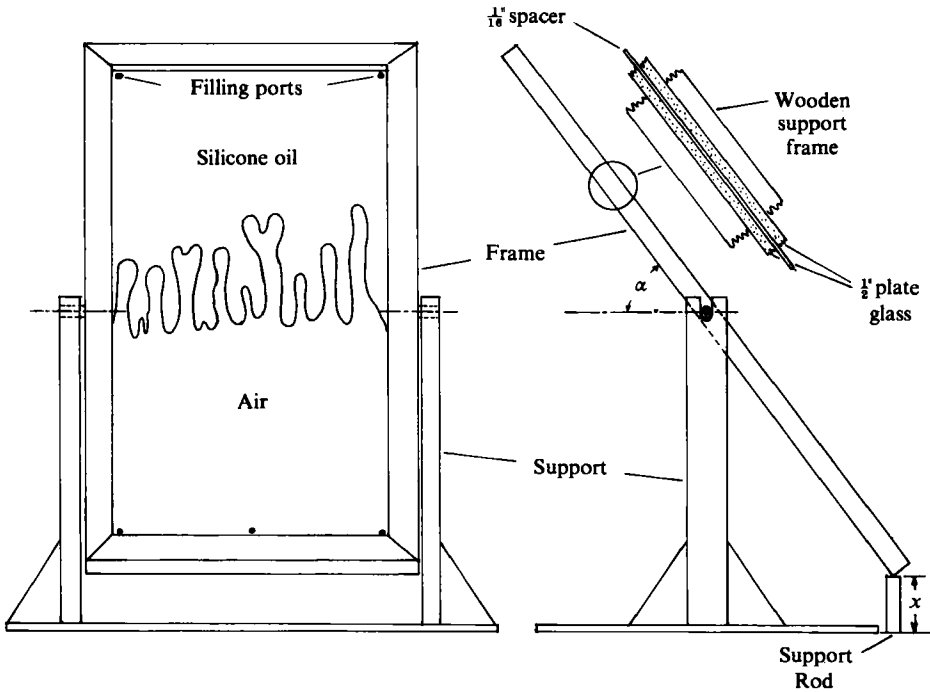


FIGURE 1. Apparatus.

the difficulty of observing the highly distorted three-dimensional interface. Use of a geometrically constrained system which forces the interface to be essentially two-dimensional, as in a Hele-Shaw cell, allows one to gain insight into the properties of the nonlinear Rayleigh-Taylor instability by using a combination of numerical calculations and experiment in an interactive fashion, i.e. tuning numerical schemes against the two-dimensional Hele-Shaw experiments and then using them to calculate the experimentally less accessible Rayleigh-Taylor system.

2. Apparatus and procedure

The basic apparatus, shown in figure 1, consisted of two 1.27 cm thick 'float-glass' plates spaced 0.21 cm apart and held in a wooden frame so that the working space was 61×120 cm. The cell could be rotated about its central, short axis and held at various pre-determined angles by supporting one end on a rod of known length. Several ports were drilled into the plates in order to fill the cell initially and to introduce other fluids, in experiments to be reported in future papers.

The interface was visualized photographically by mounting a 35 mm SLR camera on a frame which was rigidly attached to the cell so that it rotated with it. The cell was back-lit by projecting the light from photographic lamps onto a translucent screen taped to the back face of the cell.

For the experiments to be reported here two immiscible fluids were used, a silicone oil, with nominal viscosity of 100 cs, and air. Clearly a large number of other possible combinations exist and the results of experiments using some of them will be presented in future publications.

In our first attempts to look at the stability of an initially plane interface the cell was filled a little more than half-full with the silicone oil. It was then rotated to a

known angle α (fig. 1) and with the heavy oil above. In this case, under all circumstances, the interface first became unstable at its two ends. This occurred because the menisci which formed there acted as very large perturbations while the transverse meniscus (i.e. that which spans the narrow gap between the two plates) was extremely rigid and unyielding and had to be released in some way in order to obtain instability along the whole length of the interface. The most successful technique for accomplishing this was to pre-wet the glass plates with a thin oil film. Thus the preliminary experiment initiated above was allowed to continue so that the oil now filled the lower half of the cell. After about half an hour most of the oil had drained from the plates leaving only a thin film behind. This procedure ensured that in all cases the interface contact angle was zero and that contact angle hysteresis was not involved in determining the stability properties of the interface. The cell was then rotated back to an angle α again with the heavy oil above, so that a distribution of instability waves was formed with a more-or-less uniform wavelength (figures 2*a*, 3*a*), allowed to grow, and then photographed. This procedure of tilting, draining and re-tilting was repeated six times for each angle of interest in order to obtain sufficient statistical information on a system which did not give exactly the same interface development in each test. In particular the evolving fingers appeared to follow no preferred paths and there were no imperfections in the plates to form centres from which growth could be instigated.

The fluid properties of significance, the surface tension T , kinematic viscosity ν and density ρ_1 , were measured at the temperature at which the experiments were performed (21 °C) and had values of $T = 21.0 \pm 0.4$ dynes/cm measured using a ring tensiometer, $\nu = 1.11 \pm 0.03$ cm²/s using an Ostwald viscometer and $\rho_1 = 0.96$ gm/cm³. It was assumed that the viscosity and density of the air were insignificant compared with those of the oil.

3. Theory

Here we follow the linear theory developed by Saffman & Taylor (1958), among others, in order to present the scaling laws that appear to be relevant to our problem and which help to explain some of the nonlinear phenomena that we have observed.

If one considers that stability of a plane interface between two immiscible fluids to two-dimensional disturbances under the influence of an imposed pressure difference which produces a uniform interfacial velocity V , and gravity, then the growth rate σ of these perturbations is given by

$$\frac{12\sigma}{b^2}(\mu_1 + \mu_2) = \frac{2\pi}{L} \left\{ \frac{12V}{b^2}(\mu_1 - \mu_2) + g(\rho_1 - \rho_2) \sin \alpha \right\} - \frac{8\pi^3 T}{L^3}, \quad (1)$$

where L is the wavelength of the disturbance, b the width of the gap between the plates, T the surface tension between the two fluids, μ the fluid viscosity and ρ the fluid density, while the subscripts 1 and 2 refer to the upper and lower fluids respectively. Here it has been assumed that the pressure drop across the interface is given by $T(2/b + 1/R)$, where R is the radius of curvature of the interface projected onto the plane of the plates. There has been a great deal of discussion in the literature concerning this assumption especially in view of the known variation of the interface transverse curvature (i.e. that across the gap between the plates) with capillary number $Ca = V\mu/T$ as calculated to first order in Park & Homsy (1984) and Park *et al.* (1984). These possibilities are mentioned again later when we discuss our results (§5).

Case	α	L^* (cm)	U^* (cm/s)	t^* (s)	B^*
V	90°	1.62	2.38	0.68	0.026
A	16.4°	3.05	0.67	4.54	0.05
B	11.1°	3.70	0.48	7.75	0.061
C	5.8°	5.13	0.24	21.5	0.084
D	3.1°	6.91	0.13	52.9	0.110

TABLE 1. Parameters of the five cases studied

From (1) it is apparent that the effect of surface tension is to limit the range of unstable disturbances to those with a wavelength greater than

$$L_c = 2\pi T^{\frac{1}{2}} b \{12V(\mu_1 - \mu_2) + b^2 g \sin \alpha (\rho_1 - \rho_2)\}^{-\frac{1}{2}}, \quad (2)$$

while the amplification factor σ is a maximum for a wavelength L^* , equal to $\sqrt{3} L_c$. This can then be used as a representative lengthscale in the data presentations which follow.

As a velocity scale we use (1) rearranged as

$$\sigma = \frac{2\pi}{L} U^* - \frac{8\pi^3}{L^3} T \frac{b^2}{12(\mu_1 + \mu_2)},$$

where

$$U^* = \frac{V(\mu_1 - \mu_2)}{\mu_1 + \mu_2} + \frac{b^2 g \sin \alpha (\rho_1 - \rho_2)}{12(\mu_1 + \mu_2)}.$$

Then a suitable timescale t^* is given by L^*/U^* . While the quantities given above are of primary importance to the presentation which follows one other important parameter appears as the result of some elementary physical considerations based upon the experimental observation of the continued instability and distortion of the few long, wide 'fingers' which evolve from the large number of initially unstable waves. The lateral growth of these fingers is apparently constrained by the presence of the sidewalls and so one would suspect that the ratio L^*/W (where W is the width of the cell (figure 5)) would be important in quantifying the ability of the fingers to support further instability.

This quantity,

$$B^* = \frac{2\pi\sqrt{3}T^{\frac{1}{2}}b}{W} \{12V(\mu_1 - \mu_2) + b^2 g \sin \alpha (\rho_1 - \rho_2)\}^{-\frac{1}{2}},$$

has the same form as the quantity $B^{\frac{1}{2}}$ of TA and is closely related to the parameter C'_a of Park & Homsy (1985), i.e. $B^{*2} = 118.4B$ and $B^{*2} = 2.47 C'_a{}^{-1}$. For future reference, we note that the commonly used capillary number $Ca = \sqrt{V\mu}/T$ is related to B^* by $B^{*2} = 9.87(b^2/W^2)(1/Ca)$.

4. Results: observation of interface evolution

We consider five cases in detail with angle α varying from 90° to 3.10°. A full tabulation of the relevant parameters is given in table 1. These angles were chosen so that L^* increased by approximately 1.5 cm from case to case. It is our objective to find useful measures of interface evolution and to see if they scale in a meaningful way; some of these have already been discussed in TA and others are trivial extensions of them. These measures will be discussed in detail in §§4.1 and 4.2. In §4.4

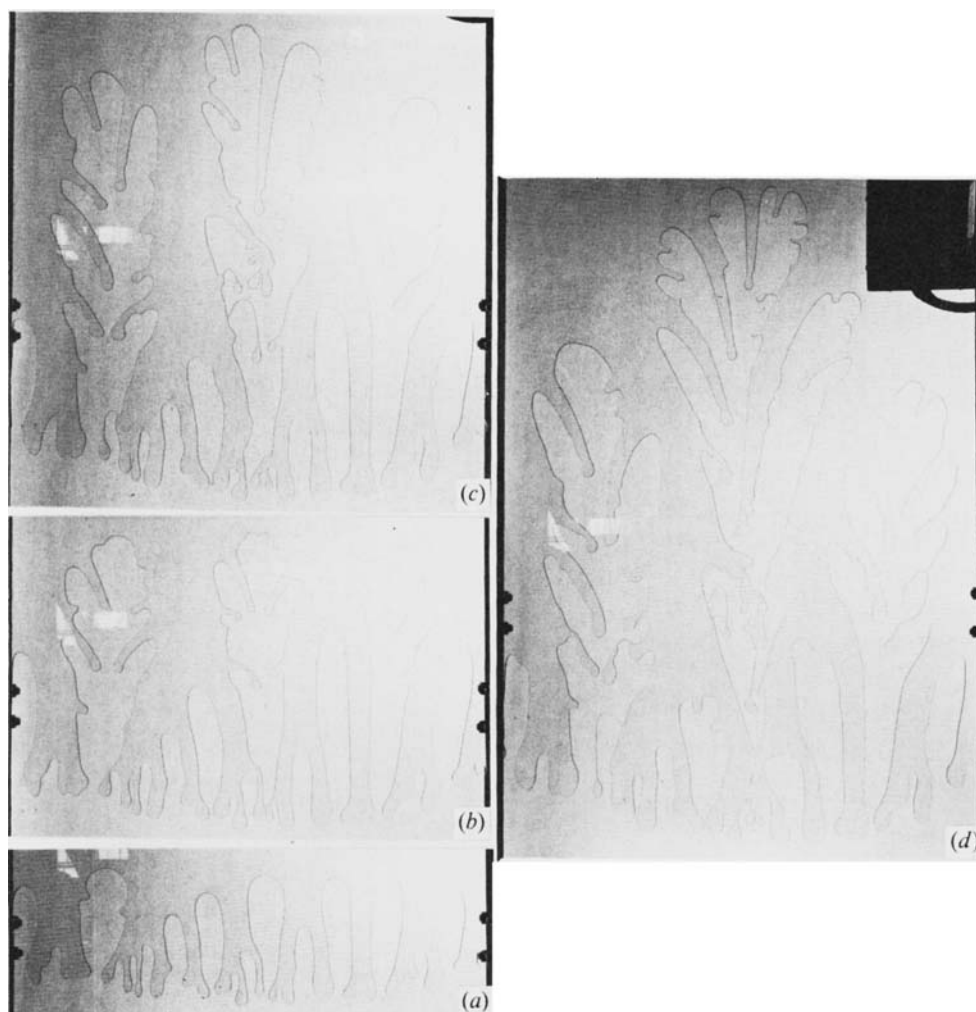


FIGURE 2. Photographs of the nonlinear development of the interface for $\alpha = 90^\circ$, case V1. Time increases from (a) to (d).

we introduce the concept of the fractal dimension of the interface as discussed in general by Mandelbrodt (1983), and in case similar to ours by Nittman, Daccord & Stanley (1985) among others.

4.1. *Measurements of the emergence of a single finger*

In figures 2 and 3 we show photographs of the complete and typical evolutionary history for two extreme cases (V and D) from the thirty sets of photographs taken and measured in detail.

For the vertical orientation (case V) a large number of small waves were formed at first but the growth of many of them was suppressed at early times so that the final stages were dominated by the growth of only three of the original wavelets with the central one ultimately out-growing and stopping the growth of its two neighbours. This process can be understood qualitatively by considering the unsteady flow field generated by the field of fingers in which one grows slightly larger than its neighbours. The flow created by this larger finger is such that it opposes the motion of these

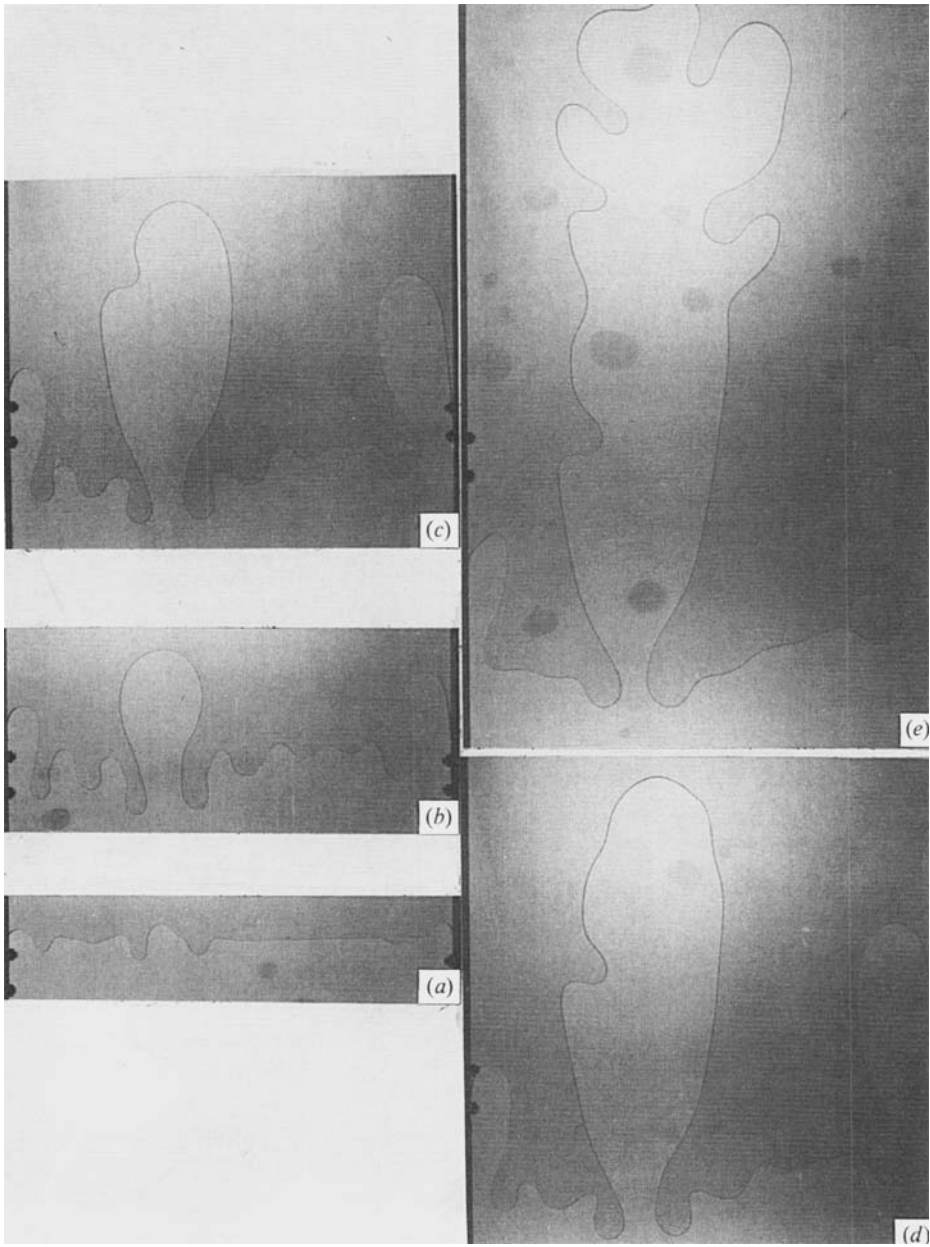


FIGURE 3. Photographs of the nonlinear development of the interface for $\alpha = 3.1^\circ$, case D. Time increases from (a) to (d).

neighbours so that they eventually, and sometimes very abruptly, stop growing (figure 4). This can be seen on rearranging (1) where we note that the gravitationally unstable interface can always be stabilized if the imposed interface velocity V exceeds $-g(\rho_1 - \rho_2)b^2 \sin \alpha / 12(\mu_1 - \mu_2)$, which certainly occurs in the cases considered here. Note, however, that as $(\mu_1 - \mu_2) \rightarrow 0$ the magnitude of V required to stabilize the interface becomes large and no stabilization takes place, as noted in TA's calculations and the experiments of Maher (1985). This process was first discussed casually by Saffman & Taylor (1958) and has been observed in a number of similar situations,

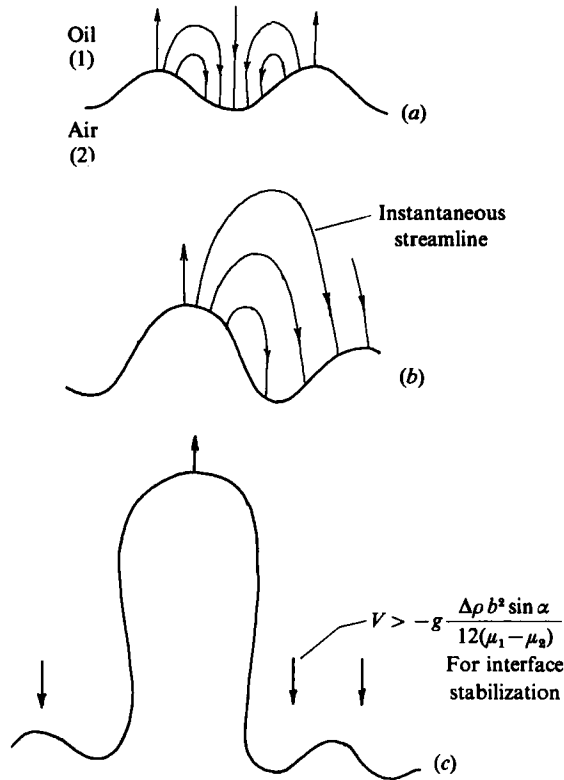


FIGURE 4. (a) Unsteady streamlines of a uniform field of growing wavelets. (b) When one wavelet becomes larger than its neighbours, owing to non-uniform initial conditions, it creates an unsteady flow field which opposes the growth of these neighbouring perturbations. (c) In the limit where the central wave, in this case, has become very large, the opposing flow is uniform and in a stabilizing direction (see (1)). This can and does suppress the growth of the smaller waves as can be seen clearly for the smaller waves of figure 2, for example.

e.g. finite-amplitude Rayleigh–Taylor instability (Emmons *et al.* 1960) and finger growth in a stratified fluid (Liu *et al.* 1985).

Ideally this process can be quantified, somewhat laboriously, by plotting the length of each individual disturbance (see figure 5) as a function of time t . Unfortunately at early times the number of growing waves was decreasing so rapidly that only a few points could be plotted. From such a plot (figure 6) it was possible to decide at what time each finger stopped growing. Thus, initially, all the waves (N) grew: after a short time t_1 one stopped growing and only $N - 1$ waves were growing. This process was repeated for all subsequent wave suppressions so that the $(N - n)$ th wave stopped growing at t_n . A plot of $\log(N - n) W/L^*$ versus $\log t_n/t^*$ yields a straight line of large negative slope (figure 7) with only one finger still growing after $t_n/t^* \approx 10$, for our particular cell. This cascade of energy to a smaller number of fingers, which then grow in width and hence to a larger scale, is very reminiscent of the upscale transfer of energy associated with the $-\frac{5}{3}$ law of two-dimensional turbulence and was, in fact, one of the motivations for studying the present problem. However it is now clear that the physical mechanisms involved are quite different, as will be discussed in §5.

Similar processes can be seen in figure 3 for case D where $\alpha = 3.1^\circ$. The initial

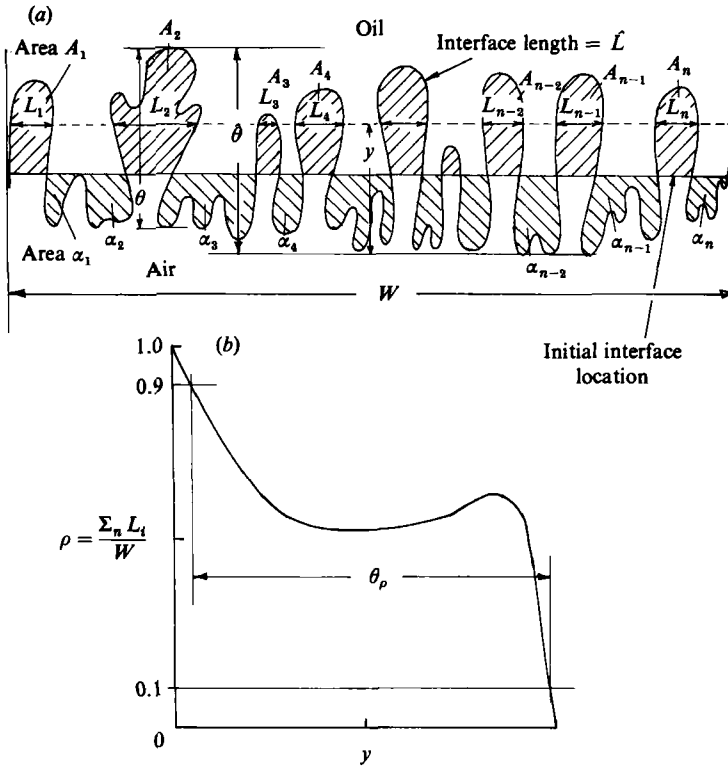


FIGURE 5. Definitions of the various quantities used in the data reduction. (a) θ is the maximum length of any individual finger; θ the maximum width of the distorted interface, \mathcal{L} is the maximum length of the interface using a map measurer (see §4.4.1). (b) The density function $\rho(y)$ is found by adding the width of each individual air finger at a specific value of y and dividing by W , a process which is repeated for many values of y . The width of the interface θ_ρ is that between $(\sum L_i)/W = 0.1$ and 0.9.

instability had a much larger wavelength and a single finger emerged very rapidly. In case V the fingers underwent many further instabilities and bifurcated many times into two or three new fingers; in case D was not the case and only a weak secondary instability could be seen. We postpone measurement and discussion of this process until later (§§4.3 and 5).

Also, a measurement of the initial number of waves N when divided into the width of the cell W gives an experimental measure of the initial instability wavelength. Since we wish to concentrate on the nonlinear behaviour of the interface and since similar measurements have been repeated extensively in the open literature (see Park *et al.* 1984 for a good discussion) we refrain from presenting them in detail here, except to note that the measured values were typically 10–15% larger than the calculated values (e.g. on figure 7 the first point representing the initial instability occurs for $NL^*/W = 0.85$). We believe that this is because it took a finite time to rotate the cell to the required angle and hence the interface began to grow, and even reached finite amplitude for cases V and A, under the action of a gravitational force that was variable and less than the final value. We are convinced, however, that this had no effect on the long-time, nonlinear growth which always took place with a constant gravitational force. It is possible, also, that an inaccuracy in measuring the gap width

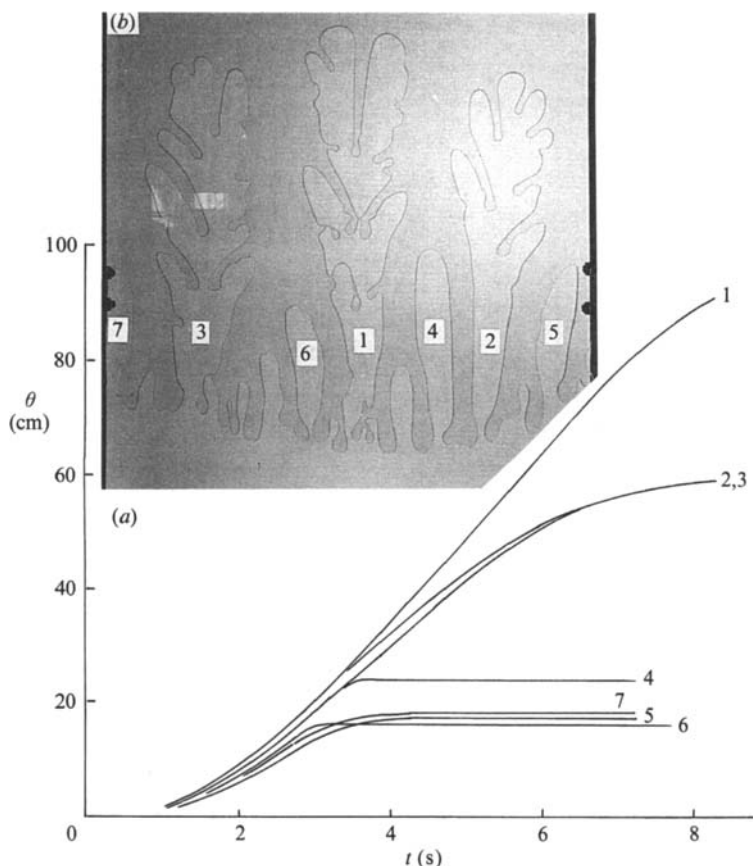


FIGURE 6. (a) Growth of the individual fingers (θ versus t) shown in (b).

b could account for some of the difference but that inaccuracies in measuring the fluid properties could not.

4.2. Measurements of interface width

One of the more practical implications of the processes shown in figures 2 and 3 is a measure of the width of the cell, in the y -direction, which has been contaminated by the growth of the interface. This is important first because it gives a quantitative indication of the time it takes for the lighter, less viscous fluid to reach the end of the cell and hence becomes less effective in displacing the more viscous fluid, in the situation of greatest practical importance (see § 1), and secondly because it determines the long-time behaviour of the interface into a parameter range where calculations have not extended so far.

This process can be characterized in several ways, as outlined in figure 5 where we define several measures of interface distortion and growth. Two integral widths can also be defined; $\theta_A = \Sigma A_i/W$ is the sum of the areas of all air fingers above the initial interface position divided by W ; $\theta_\alpha = \Sigma \alpha_i/W$ is the sum of the oil-filled areas below this line, divided by W . Three of these, $\hat{\theta}$, $\rho(y)$ and \hat{L} , have already been used by TA while the others, θ , θ_A , θ_α and θ_ρ , are trivial extensions. Of primary interest is the total maximum interface width $\hat{\theta}$. Raw-data plots for three cases are shown in

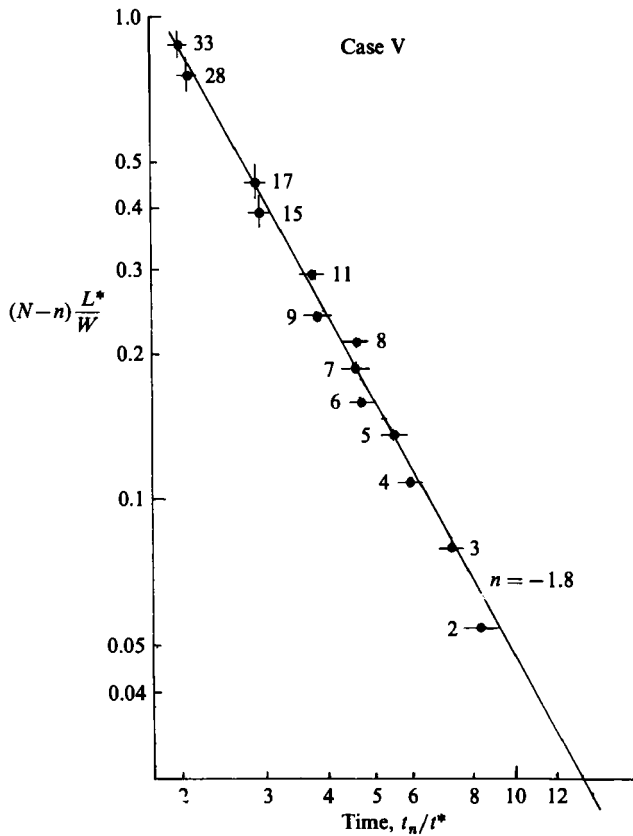


FIGURE 7. Characterization of the emergence of a small number of large fingers at experiments progress. For cases V1 and V2 we plot $(N-n) L^*/W$ versus t_n/t^* .

figure 8 for the six individual realizations of each case. The averaged result for each case is shown as a solid line. Representative points from these averaged curves are plotted in non-dimensional fashion on figure 9 for all five cases. We see that, except for the most distorted interface for the smallest value of B^* (table 1, case V), all of the cases can be reduced to a single curve using

$$L^* = 2\pi\sqrt{3} \left\{ \frac{T}{g(\rho_1 - \rho_2) \sin \alpha} \right\}^{\frac{1}{2}}, \quad t^* = \frac{2\pi\sqrt{3} \ 12(\mu_1 + \mu_2) T^{\frac{1}{2}}}{(g(\rho_1 - \rho_2) \sin \alpha)^{\frac{3}{2}} b^2}$$

as the characteristic length and time scales respectively (see §3). We suspect that this change in behaviour with decreasing B^* occurs continuously, but rapidly, over a small range of B^* . Unfortunately our strategy for choosing values of B^* , or α , for study did not include the possibility of such a rapid change. In future studies we plan to look at this effect more carefully.

Certain integral measures of the interface width can also be constructed as outlined above and on figure 5. If on any particular photograph, we draw a straight horizontal line representing the original position of the interface, then the sum of the areas A_i of the air fingers above this line, when divided by the cell width W , gives a measure of the half-width of the interface θ_A . If, in a similar fashion, we sum the areas of oil penetrating below the original interface position α_i and divide by W then a second

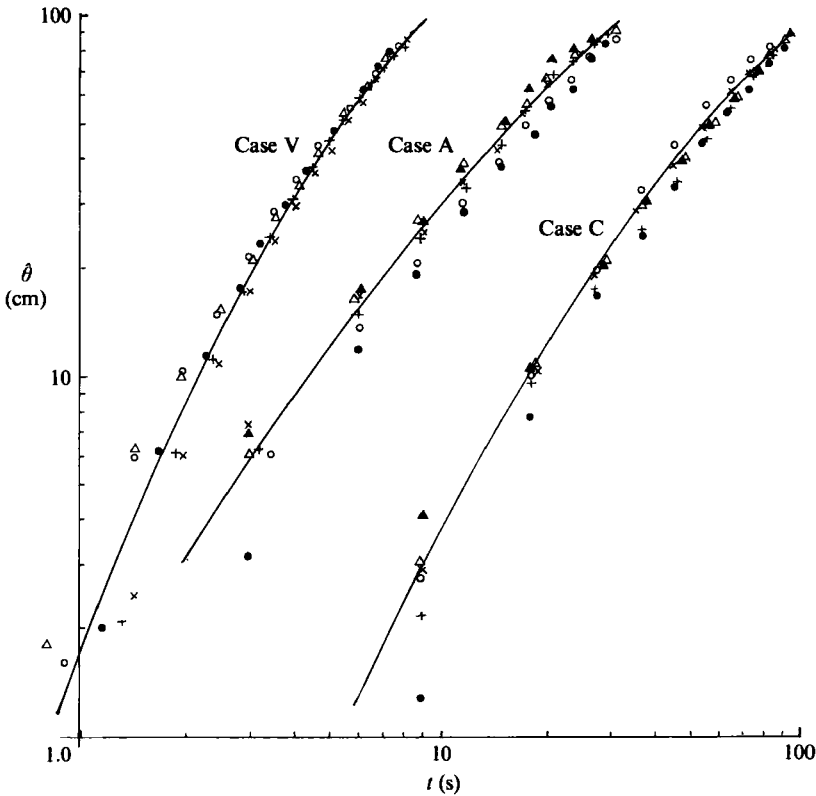


FIGURE 8. Maximum interface width $\hat{\theta}$ versus time for cases V, A and C. In each case the curves represent the average of six individual experiments.

integral width θ_α results. Any difference between the two values measures the average thickness of the oil film \bar{l} left behind as the air penetrates upwards, i.e.

$$\begin{aligned} \text{Volume of air displaced above datum line} \\ = \sum A_i(b - 2\bar{l}) = b\sum \alpha_i = \text{Volume of oil below datum line.} \end{aligned}$$

Thus

$$\bar{l} = \frac{b}{2} \left\{ 1 - \frac{\sum \alpha_i}{\sum A_i} \right\} = \frac{b}{2} \left\{ 1 - \frac{\theta_\alpha}{\theta_A} \right\}.$$

Unfortunately it did not prove possible to measure this difference in area with sufficient accuracy to determine the film thickness, as can be seen from a careful study of the results of the measurements of θ_A and θ_α displayed on figure 10.

The final measure of the interface width, θ_ρ , (figure 5b) is virtually identical with $\hat{\theta}$, except at early times, and scales in the same way (figure 11). However, the technique used to find it gives useful information about the relative distribution of oil and air within the interface, in fact the results can be considered as a measure of the density distribution ρ within the interface or alternatively the probability of being located in an air finger at any particular value of y . These distributions were found by drawing straight horizontal lines, L_i , at various y -stations within the regions filled with air. These lengths at a given value of \hat{y} were then summed and divided by W to give the density, $\rho = \sum L_i/W$ (figure 5b). Plots of ρ at approximately the same dimensionless time, are given in figure 12(a-d) for the six realizations of each of

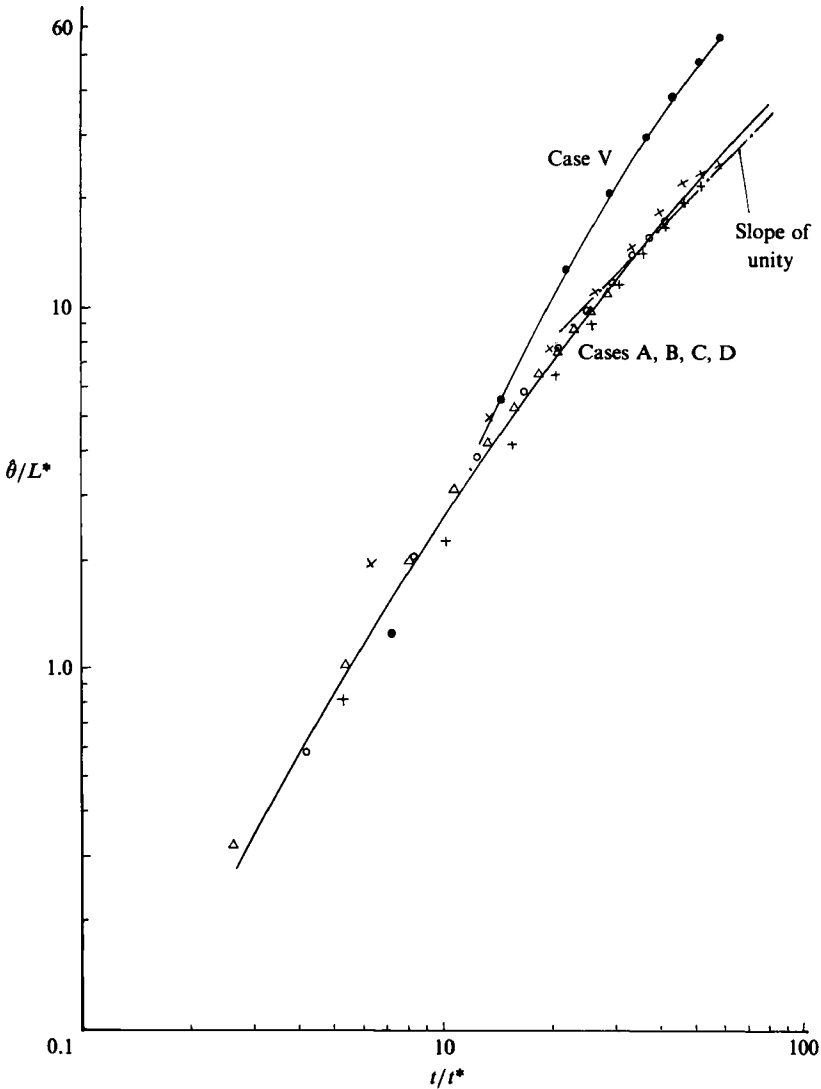


FIGURE 9. Averaged non-dimensional maximum interface width versus non-dimensional time for all five cases.

the cases A–D, while the resulting estimated averages are replotted on figure 13. Of major interest is the similarity of the curves and the fact that the cell has only slightly more air than oil over its central half, a result which is very reminiscent of the findings of Saffman & Taylor (1958), among others, who found for single smooth fingers created by injection into a horizontal cell that the cell was half filled with air for large values of a parameter equivalent to our B^* and a capillary number $V\mu/T$. The consistent rise in the proportion of air at large values of y/θ_ρ , around 0.9, i.e. towards the oil-filled side, is also of interest and has no counterpart in the single, smooth-finger experiments. This effect appears to be due to the bulbous nature of the generated fingers and is consistent with the numerical results of TA. G. Tryggvason (private communication) suggests that this effect is enhanced in numerical calculations if one assumes a dependence of the pressure drop across the interface on interface velocity,

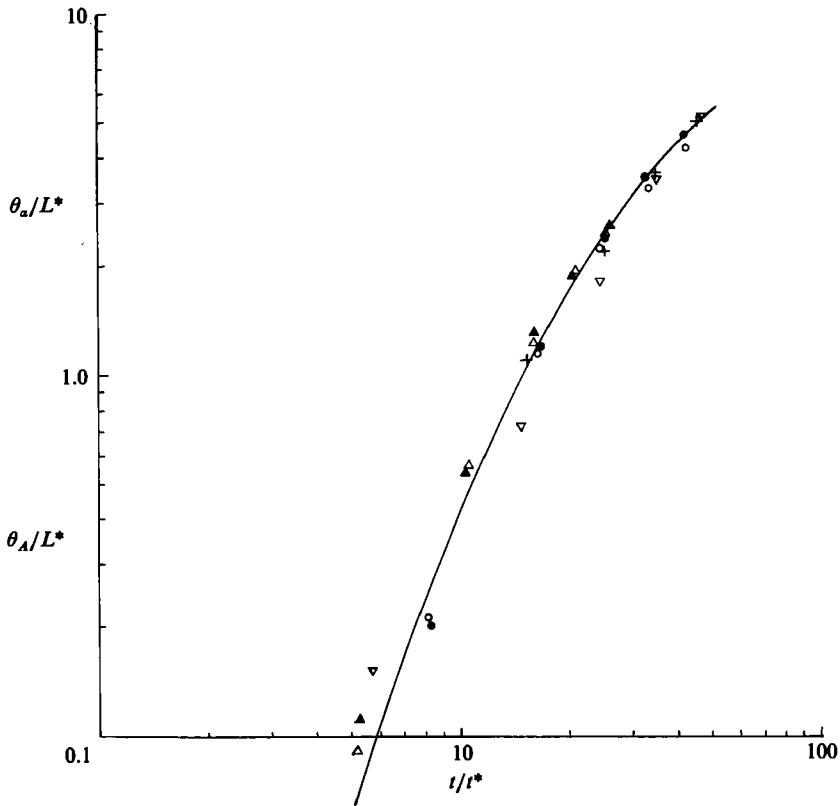


FIGURE 10. Integral measures of the interface width θ_A/L^* and θ_α/L^* versus t/t^* . θ_A/L^* : ∇ , case B; \circ , case C; \blacktriangle , case D. θ_α/L^* : \bullet , case B; $+$, case C; \triangle , case D.

but a quantitative assessment of this suggestion is lacking at the moment. It is also of interest, for our discussions later, that at longer times the shape of the ρ -distribution does not change very much with time. This we show as figure 14 where, for case A, ρ -distributions are plotted at different non-dimensional times.

The ρ -distributions for case V (figure 15) also show the marked difference between this case and cases A–D noted previously. The value of ρ in the centre of the cell is markedly lower than the value for the other cases and no rise in value is found for large values of $y/\hat{\theta}$. Such values of ρ are also typical of the single-finger results with values of $\rho < 0.5$ that were found recently by Tabeling, Zocchi and Libchaber (1986) at large Ca .

Finally, we note that all of the measurements of interface width tend to a slope of unity at large times, a result which is also consistent with the pumped-interface results of many authors on the growth of single fingers. However this result is somewhat clouded by the fact that at these larger times the fingers were approaching the end of the cell and therefore could have been affected by its presence. At early times the growth rate $d\hat{\theta}/dt$ appears to scale approximately as $t^{1/2}$, i.e. $\hat{\theta} \sim t^{1.5}$. While linear stability results would lead us to expect an exponential growth at early times, the first points of figure 9 already represent an amplitude of about half a wavelength, so that they are well outside any linear stability range. Under these circumstances an algebraic growth with time is not surprising. This result is close to that found by Maher (1985) in the same range of t/t^* ; in fact Maher's result of $\hat{\theta} \sim t^{1.6}$ is well within

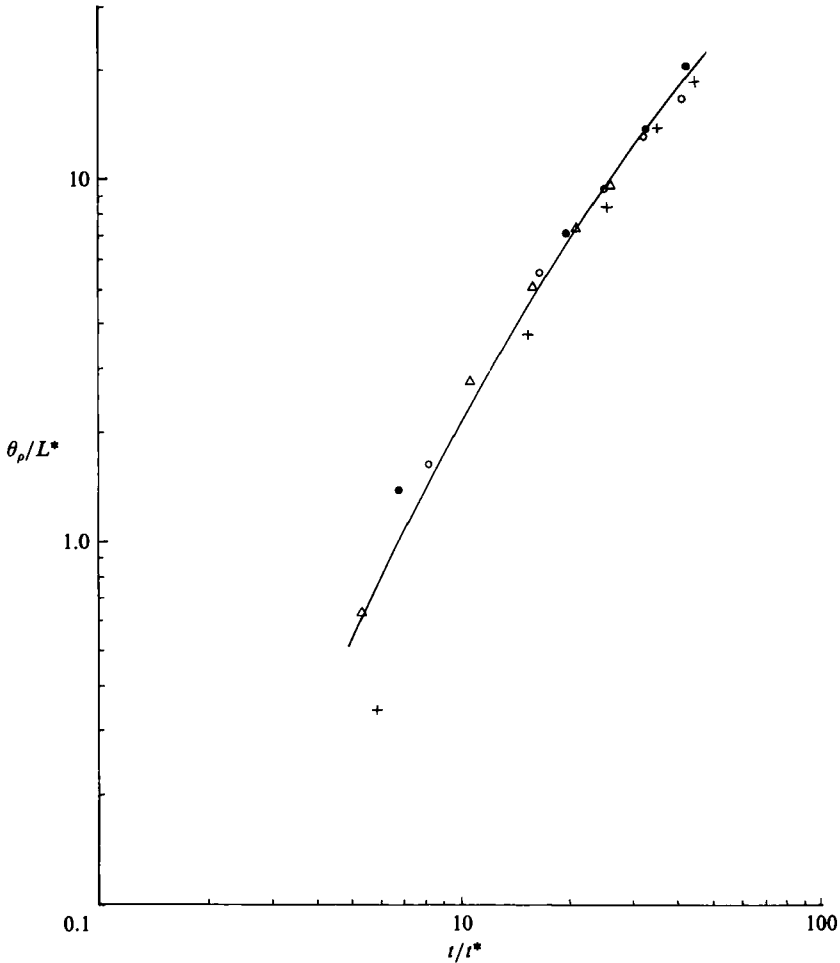


FIGURE 11. Interface width θ_ρ/L^* versus t/t^* : ●, case A; +, case B; ○, case C; △, case D.

the experimental scatter, while both have a considerably lower exponent than that found by TA.

4.3. Measurements of the interface length

For these measurements the photographic negatives were projected to one-third full size and the infacial outline traced. The interface lengths were then found by running a standard 'map-measurer' around the interface and converting to full-scale units by multiplying by measured coefficients. The average results for each case can be presented in several different ways. Following TA we plot $(\bar{L}-W)/W$ versus t/t^* in figure 16, which shows a consistent trend with decreasing B^* from case A to case D and a tendency to a linear growth with time at longer times. As with the measurements of θ , case V appears to be quite anomalous, while even the cases A–D do not reduce to a single curve, as in TA, for example, suggesting that the more distorted interfaces we have observed are different from those found in the existing numerical schemes. Alternative ways of plotting these results, which show similar trends, are displayed in figures 17 and 18. Both figures reinforce, in particular, the different behaviour of case V, while even the cases A–D which are reasonably close

to each other will still show a definite ordering with L^* or alternatively, and probably more appropriately, B^* . In figure 17, we have also plotted \hat{L}/L^* versus t/t^* for case V since this appears to have some relevance to the results that follow [§4.4.1.] and the discussion of §5.

4.4. Measures of interface distortion

4.1.1. Interface dimension

It is evident from even a casual scrutiny of the photographs displayed in figures 2 and 3 that as each major wave or finger emerged from its neighbours it underwent further instability or splitting usually, but not always, at the 'finger-tip'. When B^* was small the secondary fingers that were then formed could undergo a further splitting, a process that could be repeated several times more for the smallest values of B^* (cases V, A and B in our experimental range).

It appears that this higher-order splitting has important consequences, especially for the measurements of interface length reported in §4.3. Such measurements are significant since the interface length represents the distance over which molecular reactions could take place if the two interpenetrating fluids were chemically active, so that this length becomes a measure of the reaction rate.

While it is easy to view an interface and make a qualitative statement about its relative state of distortion it is not so easy to quantify such comments. Research on related topics (Mandelbrodt 1983) suggests that one possible way to characterize the interface distortion quantitatively is to measure, or at least attempt to measure, its dimension. We report such measurements here and although the results are not entirely unambiguous they do suggest that the concept may have some validity under some circumstances. We consider only a few cases in detail. Since case V seems to hold the most interest we present analysis of two runs from this sequence each of which had a different development. The first, which evolved clearly into a single branched finger (figure 2), we designate case V1. The second evolved into two fingers which grew at the same rate during the total period of observation (case V2). For these we consider a complete time history, while for the other cases (A–D) we present results for the final state only.

One can measure the interfacial dimension by stepping around a projected image of the interface with a pair of dividers set to a known distance, which we call the gauge length G . The number of steps N required to fit the interface when multiplied by G gives the interface length L_G at that value of G . This process is repeated for various values of G and the results plotted logarithmically. If the resulting line has a constant negative slope ($-n$) then the dimension of the interface D is $(1+n)$. One such plot is shown in figure 19 for the case V2. We note that at all times the curves quickly asymptote their values for $G=0$ for G -scales approximately smaller than L^* . Only the curves for longer times, i.e. the most branched and distorted interfaces, have an extensive region of straight negative slope for values of G from L^* to about $10L^*$, with rapid variations in L_G at larger G -scales. This is similar to results found under other, related, circumstances (Nittman *et al.* 1985, for example) and reviewed in Robinson (1985). At the shorter times the curves are definitely oscillatory and although one can draw straight lines through them the resulting values of the slopes probably have little significance. These results suggest that the interfaces may have a fractal dimension ($D = 1.44$ for case V1 and $D = 1.37$ for case V2) but that it only exists for a limited range of scales. We suspect that this range may be extended to larger values of G by allowing a longer time of evolution and many more finger bifurcations in a larger cell. It clearly cannot be extended to scales smaller than

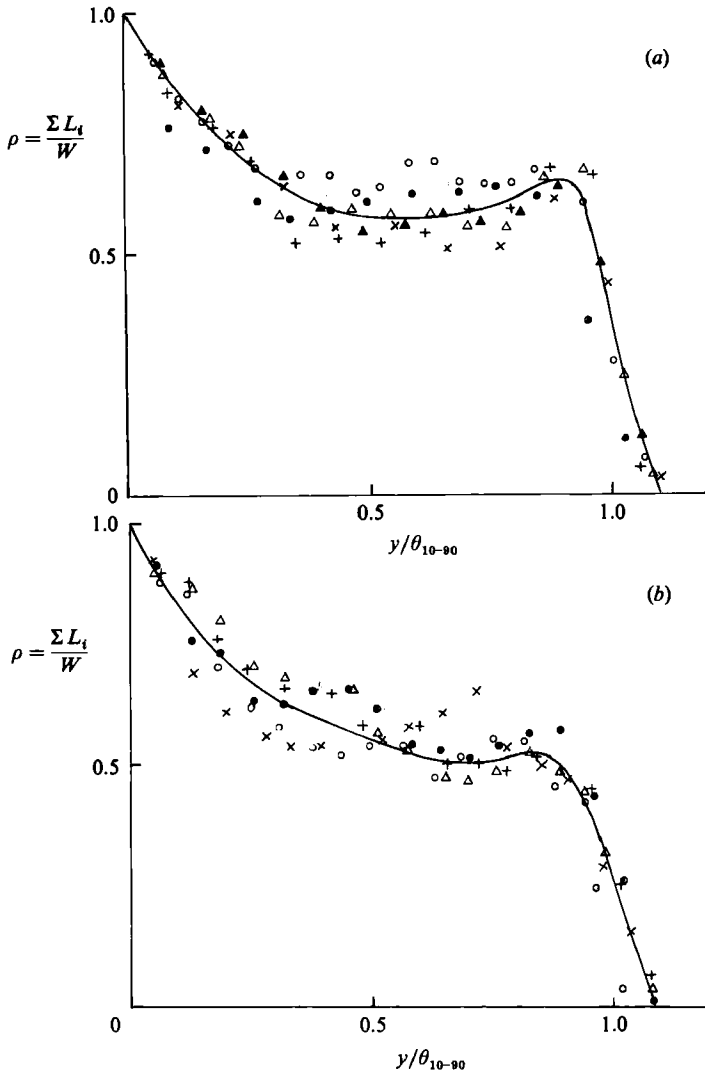


FIGURE 12(a,b). For caption see facing page.

approximately L^* since surface tension prevents smaller scales from forming. An initial report of this result has been given in Maxworthy (1985). The precise significance of these results is hard to assess at the moment. It may be coincidental that the length of the interface \bar{L} (see figure 17) grows at a power of time, 1.37, close to the values of D for these cases, so that a clear-cut region of straight negative slope may in fact distinguish the very different behaviours of the vertical cases from those where such a region is not quite so evident. The comments of Aref & Tryggvason (1984) concerning the unlikely appearance of fractal forms in this case do not seem to be borne out by these and similar experiments.

Other measurements bear out this possibility. If we plot $\log L_G$ versus $\log G$ for cases A–D for the latest times and hence most-distorted interfaces even case A, which to the naked eye has a quite complex shape, has no clear-cut region of straight negative slope, while the interface length grows approximately linearly with time. Cases B–D have quite oscillatory $\log L_G$ - $\log G$ curves and slopes of the curves of

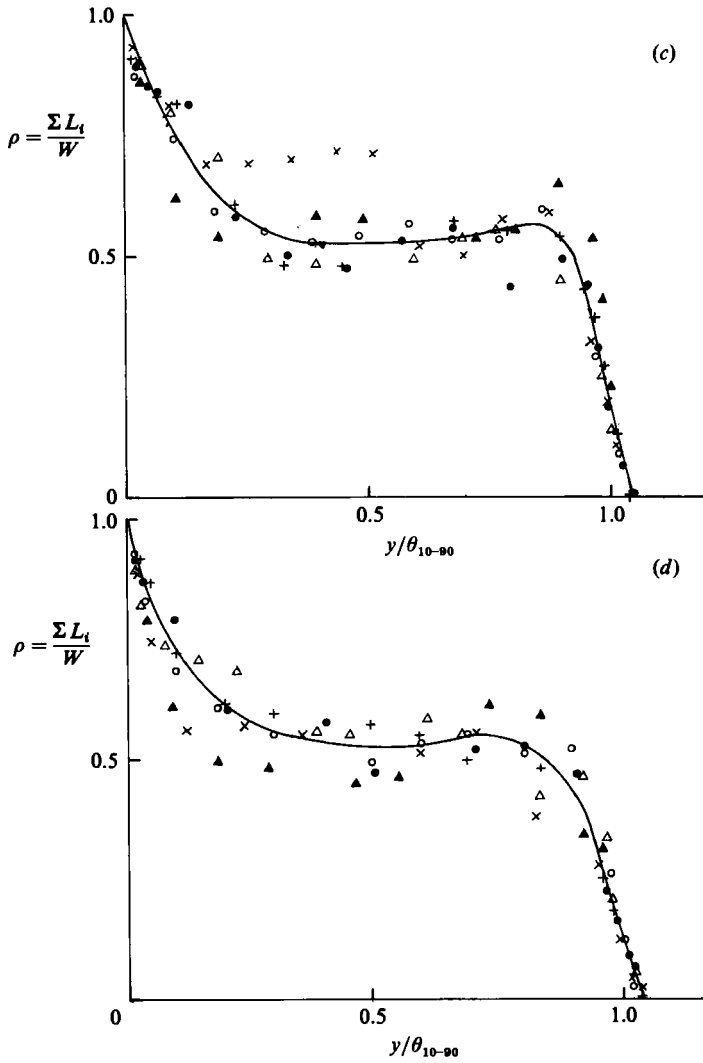


FIGURE 12. Density distribution $\rho = (\sum L_i)/W$ versus y/θ_ρ for cases A–D for six experiments in each case. (a) case A, $t/t^* = 2.0$; (b) B, 2.6; (c) C, 2.5; (d) D, 2.1.

interface length are considerably less than unity. We propose a discussion of these and other matters in §5.

4.4.2. Area-length relationships

Mandelbrodt (1983) suggests that in a system of fractal dimension there are certain useful relationships between area and length that should be observed. In figure 20, we present such relationships for case V1 (figure 2). Here interface length \bar{L} and width $\hat{\theta}$ are as discussed before (figure 5); the area, however, is different, being the total area of the air space above a line drawn through the lowest extremities of the interface.

For small times the results of figure 20 suggest that the interface is one-dimensional and similar since $A \sim L^2$. However, the long-time results are consistent with our previous observation that the effective horizontal extent of the intruding air fingers

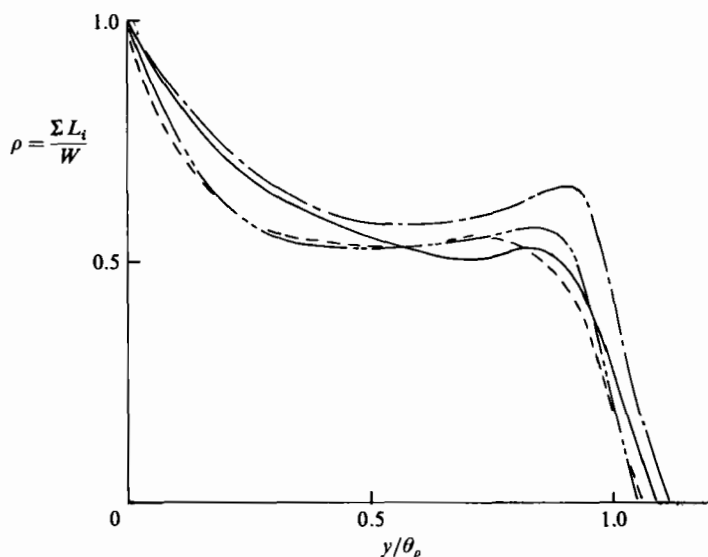


FIGURE 13. Comparison of the averaged ρ versus y/θ_ρ curves for cases A-D. —··—, case A; —, case B; — — —, case C; - - - -, case D.

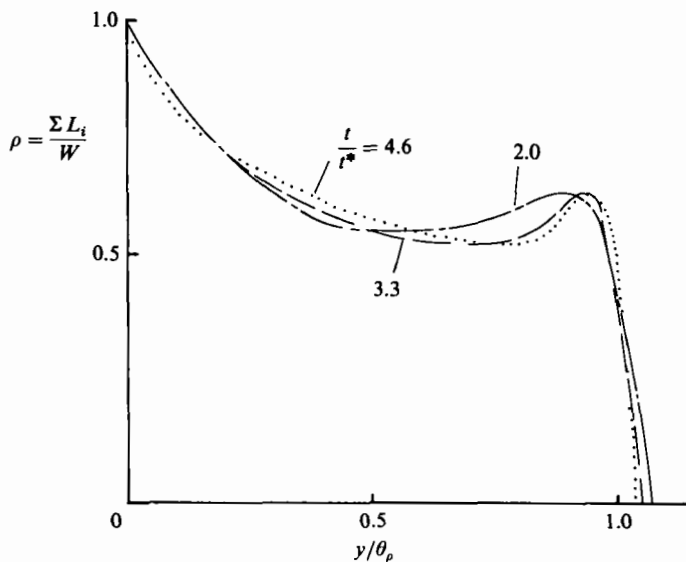


FIGURE 14. Comparison of the averaged ρ versus y/θ_ρ curves for different times for case A.

is approximately constant at a little under 50% of the total width of the cell W , figure 15. This area must eventually grow linearly with the characteristic length dimension $\hat{\theta}$ since

$$A = W \int_0^{\hat{\theta}} \rho(y) dy = W \bar{\rho} \hat{\theta} \approx \text{const } \hat{\theta}.$$

We suggest that this is probably due to the highly constrained flow produced in these experiments which quickly felt the effects of the sidewalls and produced a constant distribution of ρ and value of $\bar{\rho}$.

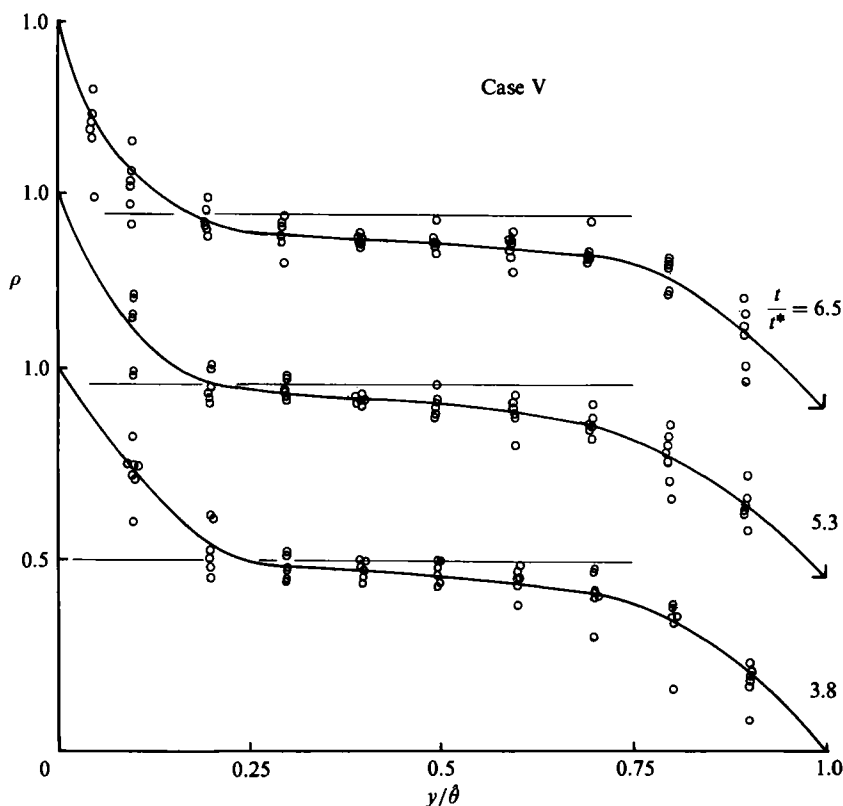


FIGURE 15. ρ versus y/δ for case V, average of seven experiments.

Mandelbrodt's (1983) results would require that $A \sim \tilde{L}^{1.43}$. Since the exponent varies from 2 to 1 in figure 20, such a region clearly exists for a short period of time, but is quickly dominated by the sidewall effects mentioned previously and cannot be considered significant.

5. Conclusion and discussion

We have run a series of experiments on the gravitational instability of an oil-air interface in a Hele-Shaw cell. We have shown how ultimately one of the initial instability wavelets grows to completely suppress the development of all the other waves and have attempted to quantify this process in a physically reasonable way by determining the times at which the various waves, which make up the initial field, are forced to stop growing by their larger neighbours. As mentioned briefly in §4.1., the growth of a smaller number of larger and larger scale features as time progresses is reminiscent of the upscale transfer of energy characteristic of two-dimensional turbulence, where a $-\frac{5}{3}$ spectrum can be justified theoretically. Unfortunately the present system probably fails as a useful analogue because of the entirely different physical processes involved. In the present case, as outlined in figure 4, the large scales grow by suppressing the growth of their smaller neighbours so that the small scales then exist virtually unchanged until the end of the experiment, and the two-dimensional motion it represents contains no vorticity. On the other hand, in the case

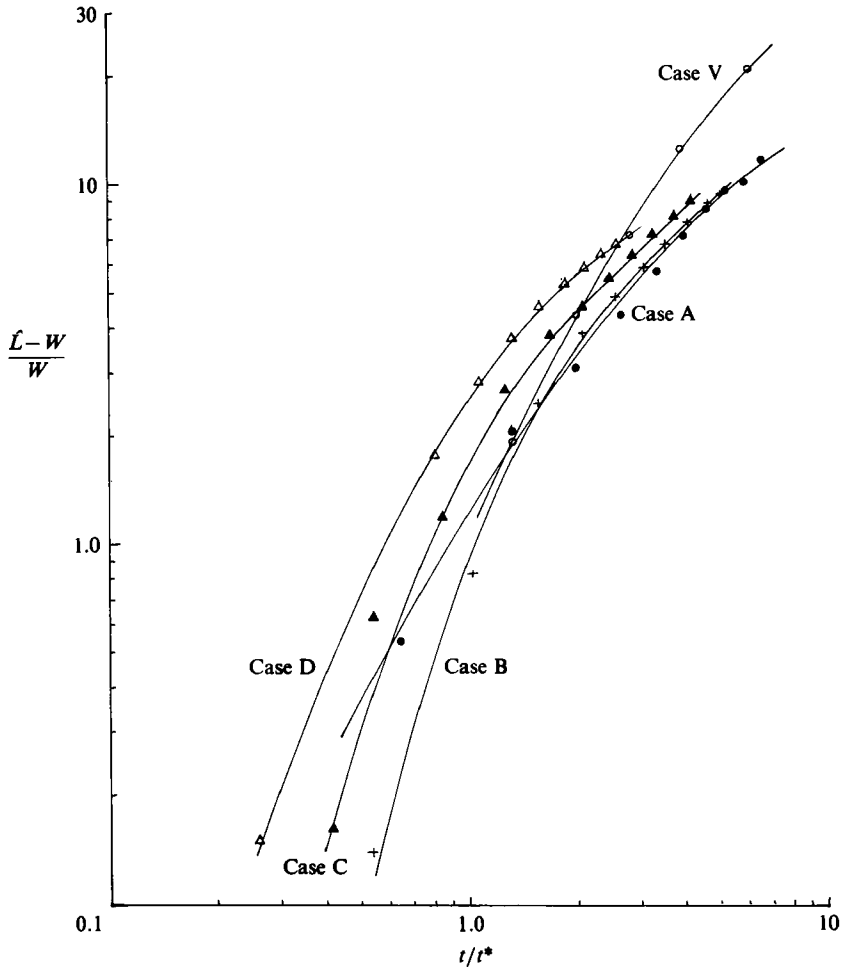


FIGURE 16. $(\bar{L} - W)/W$ versus t/t^* for all cases.

of two-dimensional turbulence large vortices grow by entraining their smaller neighbours (Caperan & Maxworthy 1985) so that eventually all the vorticity is contained in a large vortex and the smaller-scale eddies disappear as separate entities.

One of the more interesting consequences of the dominance of a few long, wide fingers that tend to fill about half of the width of the cell is that they can become so large that they, in turn, can become unstable to a combined gravitational-displacement instability. Here, not only is the gravity field destabilizing, but the fact that the less viscous fluid (air) is displacing the more viscous (oil) means that the growth rate of any secondary perturbation is enhanced (equation (2)). In fact for typical parameter values for case V the contribution of the first term in the bracket of (1) is two to three times larger than the second. We assume that the transverse curvature of the surface with a sign opposite to that with which the instability grows has some non-negligible effect on both the growth rate and instability wavelength, but this effect has not been calculated theoretically, although some numerical (DeGregoria & Schwartz 1986) and experimental (Park & Homsy 1985) work has been

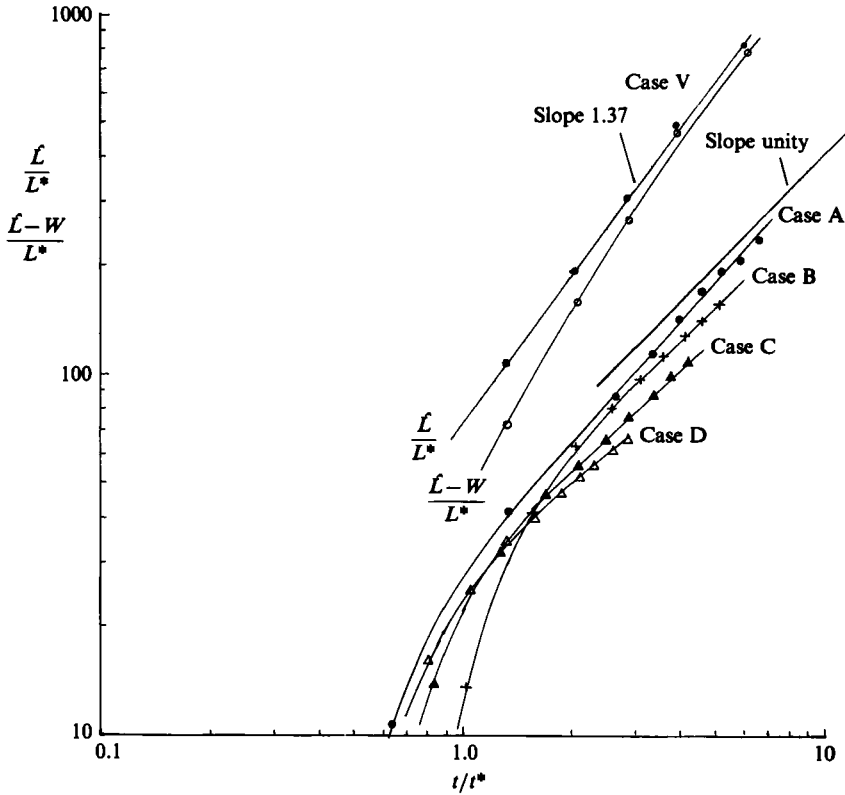


FIGURE 17. $(\bar{L}-W)/L^*$ versus t/t^* for all cases, and, \bar{L}/L^* for case V.

carried out on this problem. That this curvature effect is important can be estimated as follows, again for case V. For gravitational instability alone $L^* = 1.6$ cm (table 1), but this value is reduced to about 0.8 cm based on a typical, measured finger velocity and using (1) for a plane interface. The observations show that the fingers undergo an instability at a wavelength not too different from the original value L^* . This suggests that the curvature of the finger tip has a stabilizing effect and increases the wavelength of instability over that found for a flat interface under otherwise identical circumstances.

The fact that highly bifurcated interfaces, such as ours, have not been seen before can be explained by observing that our values of B^* are substantially smaller than those previously considered. Thus, Saffman & Taylor (1958) experimented at values greater than about 0.24 (but see comment below) and Park *et al.* (1984) at values larger than 0.14. More recently Park & Homsy (1985) have found instability for values smaller than about 0.15, where they observe the start of a tip-splitting process. Tabeling *et al.* (1986), have found instability for $B^* < 0.13$, with a measurable sensitivity to the homogeneity of the gap b . Maher's (1985) minimum value of B^* was about 0.22 and he found no instability. Comparison with the results of TA shows that two of their figures (3f and 4) have a value of $B^* = 0.15$ and should be stable; on the other hand their figure 7 has a $B^* = 0.036$ and should show some sign of higher-order instability, but it does not. DeGregoria & Schwartz (1986) find instability at $B^* \approx 0.17$ but suggest that instability could occur at even larger values if the initial distortion of the interface is large enough. Such ramified structures

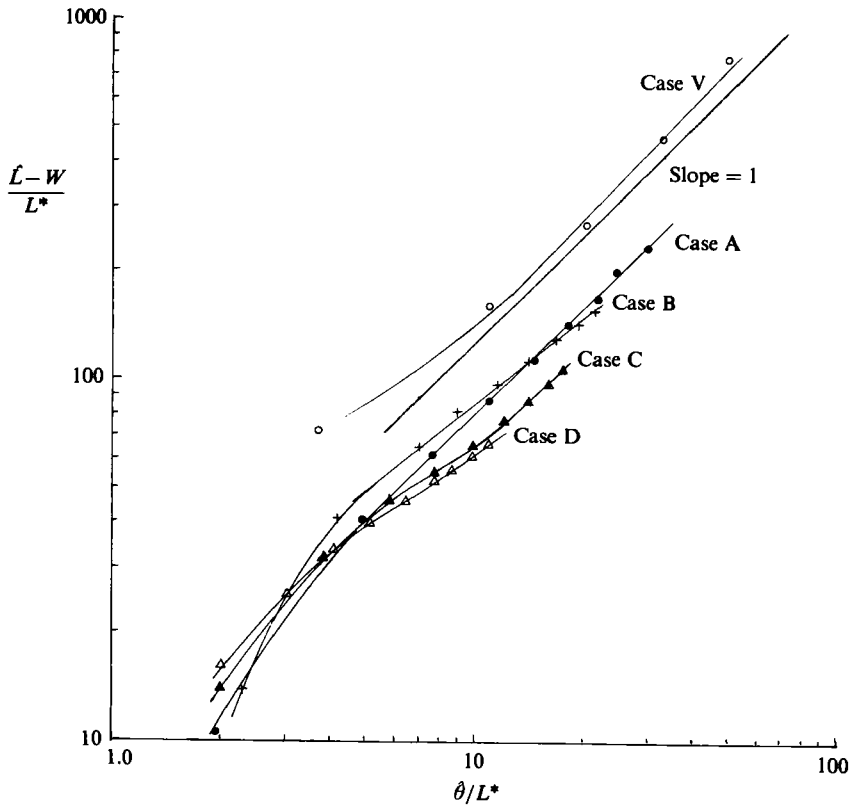


FIGURE 18. $(\bar{L} - W)/L^*$ versus θ/L^* for all cases.

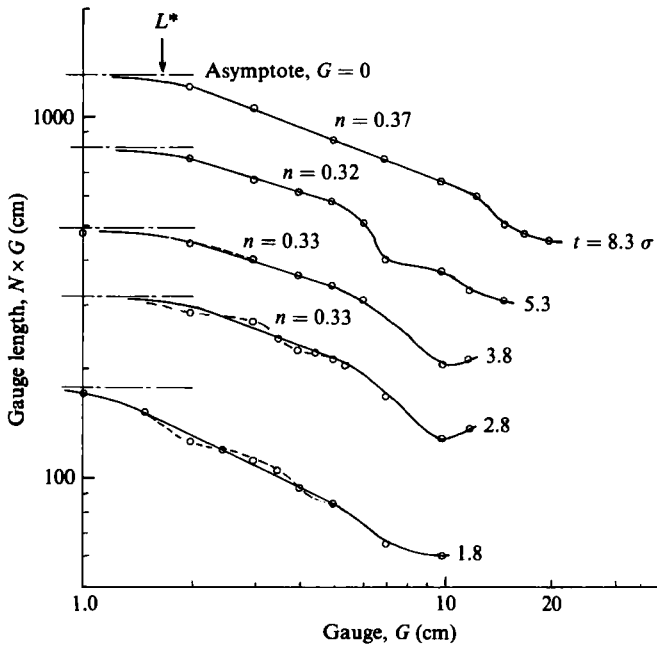


FIGURE 19. Interface length as measured with a certain gauge length G versus the value of G itself for case V2 at various times during the evolution of the interface.

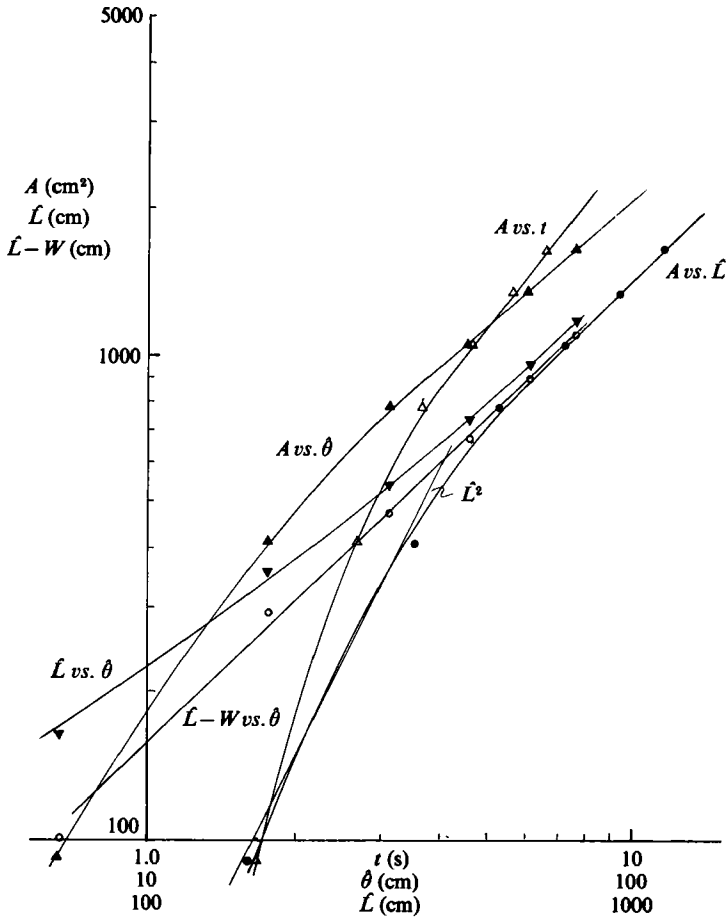


FIGURE 20. Area-length relationships for case V1.

have also been found by Liang (1985) in numerical simulations for small T . In our case, fingers grow to such a large size that at small B^* their dimensions easily exceed any modified value of L^* and further instability is possible. This explanation is further enhanced by noting that the effective modified value of B^* for our rapidly growing, large-amplitude fingers is smaller by a factor of about two than the values calculated in table 1 for gravitational instability alone, when the measured velocity of finger advance is used. Finally, a careful reading of Saffman & Taylor (1958, page 323, last two lines), suggests that they saw such instabilities too but chose not to pursue their study in depth.

The growth of the width of the distorted interface has been measured as has the change in interfacial length. In both cases it appears that the most distorted interfaces, for the smallest value of B^* , behave differently from the other cases, which appear to scale with L^* and t^* . We have attempted to quantify this difference by calculating the dimension of the interface and find that a fractal dimension of about 1.4 can be assigned to the most distorted interfaces but only for scales larger than L^* . For the other cases, the existence of a fractal dimension is doubtful and this is, we suspect, is the reason for the different behaviour of the interface in these cases. Recently Nittman, *et al.* (1985) have calculated the fractal dimension of a physically

similar system to the one we present here. In their case, through careful choice of the intruding fluid, they were able to produce an interfacial instability for which L^* was very small. The highly distorted and branched interface they have photographed had a fractal dimension of 1.36, close to the value we have calculated for the same value of B^* . The present results suggest that one might use the concept of the fractal dimension to learn something about the interface evolution. In particular, there is some evidence to suggest that the interface length grows with time to a power equal to the dimension. If this result proves to be true under further scrutiny it would constitute a powerful and useful result which could, hopefully, be extended to higher-dimensional systems since it is directly related to the area over which a reaction would take place in a cell containing reacting fluids. For reasons that probably have to do with the laterally constrained nature of the present experiments, the area-length relationship presented by Mandelbrodt (1983) is obeyed only over a restricted range. This can be explained by noting that the dimensionless density distribution ρ within the interface region does not change much after a short time and hence that the area of the intruding air 'fingers' must be linearly related to the width of the interface $\hat{\theta}$ (§4.4.2). Thus similarity arguments, on which Mandelbrodt's results depend, do not hold at long times.

The theory and virtually all of the experiments presented here have been interpreted as if the interface were a simple discontinuity across which there was a jump in pressure, as given in §3 or as modified by Park & Homsy (1984). In reality the conditions at the interface are far more complex, being the result of balance between viscous \mathcal{V} , surface-tension S , inertia I and gravitational G forces. A simple dimensional analysis reveals that under most circumstances I can be ignored, i.e. $Re = Vb/\nu \ll 1$. Generally G has been ignored in previous work also, but, in fact, $G/\mathcal{V} = (g\Delta\rho/\rho)(b^2/V\nu)$ is large and $G/S = \Delta\rho gb^2/T$ is order one, typically, where $\Delta\rho$ is the density jump across the interface. Finally $\mathcal{V}/S = V\mu/T = Ca$, and this has been considered as the major control parameter. In particular the thickness of the film left behind on the plates should depend strongly on Ca (see Reinelt & Saffman 1985 for a recent discussion) and we suspect that some dependence on $g\Delta\rho b^2/\rho V\nu$ will be found in detailed future measurements. It is also likely, for the types of curved interface found in these studies, that this film will have a variable thickness across the width of a finger-like intrusion. It has been suggested that it is, in fact, the normal velocity at a curved interface V_N that should be used to calculate a modified or local $Ca_N = V_N \mu/T$. That this cannot be entirely correct can be deduced by noting that the observed film thickness does not go to zero at the sides of fingers where $V_N = 0$, at least for the relatively large values of Ca considered here. However, recent experiments by Tabeling & Libchaber (1986) show such a variation in thickness for $Ca < 3 \times 10^{-3}$ upon *assuming* that the film thickness is zero when $V_N = 0$. In our experiments with many fingers all growing at different rates the local values of Ca cover a wide range, from essentially zero to 0.3 for the fastest moving fingers. This variation and the concomitant variation of film thickness accounts for the streaky nature of the film observed visually and in the photographs of Maxworthy (1985). In turn this means that the interfacial boundary conditions must vary along the interface, a state of affairs that has not been considered theoretically, except to first order (Park & Homsy 1984), but must be characteristic of any experiment. The importance of this in determining the stability of the interface is presently the centre of much debate and while the present experiments do not address this question directly they do provide a point of view from which to attack this problem in the future.

One can also observe in figure 2, and Maxworthy (1985), a number of filamentary structures evolving with the ratio of their width to b of order one, within which three-dimensional effects must be important and which sometimes rupture. These are invariably relatively passive structures and do not contribute to the major dynamical properties of the interface which are controlled by the growing fingers and the superimposed perturbations, all of which are at least an order-of-magnitude wider than the cell gap width. The filaments have their counterparts in the calculations of TA but there, of course, no algorithm to allow rupturing is incorporated. There are also regions where adjacent interfaces combine to form a new surface alignment, an effect which has not yet been incorporated into existing numerical schemes.

The help of J. Puddington, W. Haby and A. Bleeker in gathering and analysing the present data is gratefully acknowledged. The work was supported by the Fluid Dynamics and Oceanography Branches of the ONR.

REFERENCES

- AREF, H. & TRYGGVASON, G. 1984 Vortex dynamics of passive and active interfaces. *Physica* **120**, 59–70.
- BENSIMON, D., KADANOFF, L. P., LIANG, S., SCHRAIMAN, B. I & TANG, C. 1985 Viscous flow in two dimensions. Preprint. J. Franck Inst., University of Chicago.
- CAPERAN, P. & MAXWORTHY, T. 1985 Experiments on two dimensional turbulence in a stratified fluid. *Proc. French Physical Society*, Nice, Sept.
- DEGREGORIA, A. J. & SCHWARTZ, L. W. 1986 A boundary-integral method for two-phase displacement in Hele-Shaw cells. *J. Fluid Mech.* **164**, 383–400.
- EMMONS, H. W., CHANG, C. T. & WATSON, B. C. 1960 Taylor instability of finite surface waves. *J. Fluid Mech.* **7**, 177–193.
- LIANG, S. 1986 Random walk simulation in Hele-Shaw cells. *Phys. Rev. A* **33**, 2663–2674.
- LIU, Y. N., MAXWORTHY, T. & SPEDDING, G. 1985 The collapse of a turbulent front in a stratified fluid. Part 1. Nominally two dimensional evolution in a narrow tank. *IUTAM Mtg on 'Turbulence in Stratified Fluids'*, Margaret River, W.A., Sept. 1985. Also submitted to *J. Geophys. Res.*
- MAHER, J. V. 1985 Development of viscous fingering patterns. *Phy. Rev. Lett.* **54**, 1498–1501.
- MANDELBRODT, B. 1983 *The Fractal Geometry of Nature*. W. H. Freeman and Co.
- MAXWORTHY, T. 1985 A note on the non-linear growth of a gravitationally unstable interface in a Hele-Shaw cell. *Phys. Fluids* **28**, 2637.
- MCLEAN, J. W. & SAFFMAN, P. G. 1981 The effect of surface tension on the shape of fingers in a Hele-Shaw cell. *J. Fluid Mech.* **102**, 455–469.
- NITTMAN, J., DACCORD, G. & STANLEY, H. E. 1985 Fractal growth of viscous fingers: quantitative characterisation of a fluid instability phenomenon. *Nature*, **314**, 141–144.
- PARK, C.-W., GORELL, S. & HOMSY, G. M. 1984 Two-phase displacement in Hele-Shaw cells: experiments on viscously driven instabilities. *J. Fluid Mech.* **141**, 257–287.
- PARK, C.-W. & HOMSY, G. M. 1984 Two phase displacements in Hele-Shaw cells: theory. *J. Fluid Mech.* **139**, 291–308.
- PARK, C.-W. & HOMSY, G. M. 1985 The instability of long fingers in Hele-Shaw flows. *Phys. Fluids* **28**, 1583–1585.
- REINELT, D. A. & SAFFMAN, P. G. 1985 The penetration of a finger into viscous fluid in a channel or a tube. *SIAM. J. Sci. Stat. Comput.* **6**, 542–561.
- ROBINSON, A. R. 1985 Fractal fingers in viscous fluids. *Science* **228**, 1077–1080.
- SAFFMAN, P. G. 1959 Exact solutions for the growth of fingers from a flat interface between two fluids in a porous medium. *Q. J. Mech. Appl. Maths* **12**, 146–150.

- SAFFMAN, P. G. & TAYLOR, G. L. 1958 The penetration of a fluid into a porous medium or Hele-Shaw cell containing a more viscous fluid. *Proc. Roy. Soc. Lond. A* **245**, 312–329.
- TABELING, P. & LIBCHABER, A. 1986 Film draining and the Saffman–Taylor problem. *Phys. Rev.* **A33**, 794–796.
- TABELING, P., ZOCCHI, G. & LIBCHABER, A. 1986 An experimental study of the Saffman–Taylor problem. Preprint, James Franck and E. Fermi Insts., University of Chicago.
- TAYLOR, G. I. & SAFFMAN, P. G. 1959 A note on the motion of bubbles in a Hele-Shaw cell and porous medium. *Q. J. Mech. Appl. Maths.* **12**, 265–279.
- TRYGGVASON, G. & AREF, H. 1983 Numerical experiments on Hele-Shaw flow with a sharp interface. *J. Fluid Mech.*, **136**, 1–30.
- WOODING, R. A. & MOREL-SEYTOUX, H. J. 1976 Multiphase fluid flow through porous media. *Ann. Rev. Fluid Mech.* **8**, 233–274.